PHYSICAL REVIEW B VOLUME 60, NUMBER 3 15 JULY 1999-I

Local-density-approximation prediction of electronic properties of GaN, Si, C, and RuO_2

G. L. Zhao, D. Bagayoko, and T. D. Williams
Department of Physics, Southern University and A & M College, Baton Rouge, Louisiana 70813

(Received 10 July 1998; revised manuscript received 26 October 1998)

We present calculated electronic properties of gallium nitride (GaN), silicon (Si), diamond (C), and ruthenium dioxide (RuO_2). We implemented a simple computational procedure that avoids a recently identified basis set and variational effect. This effect, inherent to the use of basis sets in variational calculations, is believed to have affected *ab initio* calculations of electronic properties of semiconductors since their inception. We employed *ab initio*, density-functional calculations using a local-density-approximation potential and the linear combination of atomic orbital formalism. There is an excellent agreement between our findings and experimental results. In particular, the calculated, direct, minimum band gap of GaN, for low temperatures, is 3.2 eV, while the practical band gap, as per the calculated density of states, is 3.40 eV. Band gaps and excitation energies for silicon and diamond compare favorably with experimental results.
[S0163-1829(99)11727-2]

I. INTRODUCTION

Local-density approximation (LDA) calculations for semiconductors, until very recently,[1,2] often led to band gaps that are typically 30–50 % smaller than the experimental values.[3,4] The discrepancies between LDA and experimental results have been mostly ascribed to limitations of the local-density approximation. The quasiparticle calculations of Rubio *et al.*[3] provide energy bands and a band gap for wurtzite GaN that agree with experiment. The dressed Green function (G) and screened Coulomb interaction (W) approach of these authors, i.e., the GW method, used nonlocal, energy-dependent, non-Hermitian operators, which are beyond density-functional theory. The essential differences between the GW results and those of previous LDA calculations are mainly between the conduction (unoccupied) energy bands obtained by the two approaches. There is a reported, surprising agreement, however, between LDA and GW results for the wave functions of the valence (occupied) bands. A recent attempt to remedy the reported failure of LDA for the conduction bands of semiconductors consists of the work of Vogel *et al.*[4] These authors employed pseudopotentials that included self-interaction corrections (SIC) and self-interaction and relaxation corrections (SIRC) in an otherwise local-density potential calculation. They obtained wurtzite GaN band gaps of 1.7 and 4.0 eV with a standard LDA pseudopotential calculation and a new pseudopotential, LDA calculation with self-interaction and relaxation corrections, respectively. Vogel *et al.* utilized the Ceperley and Alder form of local-density approximation as parametrized by Perdew and Zunger.[5]

Recently, Bagayoko and co-workers identified[1,2,6] a basis set and variational effect inherently associated with the use of the linear combination of atomic orbital (LCAO) or linear combination of Gaussian orbital (LCGO) formalism in variational calculations of the Rayleigh-Ritz type. Essentially, the effect consists of a possible lowering of some unoccupied energy levels or bands for molecules, clusters, or solids, on account of a mathematical fact.[7,8] This fact is stated in the theorem[7] that describes the lowering or unchanged feature of any variational eigenvalue as the size of the basis set, i.e., the dimension of the matrices in the eigenvalue equation, increases. The theorem simply asserts that a given variational eigenvalue upon an increase of the size of the basis set is never increased, and that it remains either unchanged (i.e., if it is equal to the corresponding exact eigenvalue of the matrix) or it is lowered to approach the exact eigenvalue from above. The extent to which such exact eigenvalues are close to their corresponding eigenenergies of the physical system under study depends on the basic theory and the approximations utilized in the process of generating the matrix. Bagayoko and co-workers[1,2] identified the basis set and variational effect that consists of any lowering of unoccupied energy levels or bands beyond that which occurred before the ‘‘convergence’’ of the occupied levels with respect to the size of the applicable basis set. The possible, unphysical nature of such a lowering, they stated, stems from the use of the wave functions—of occupied states only—in constructing the charge density and the potential from one iteration to the next.

Bagayoko *et al.*[2] successfully applied the Bagayoko, Zhao, and Williams (BZW) procedure,[1] described below, to circumvent methodically the above basis set and variational effect while avoiding any possible ‘‘incomplete’’ nature of the basis set. Their calculated electronic and optical properties of $BaTiO_3$ agree very well with experimental results. The universal nature of the above mathematical theorem naturally raised the question whether or not the reported limitations of LDA, particularly as they pertain to the description of unoccupied energy levels or bands, are due to LDA or to the manifestation of the above basis set and variational effect.

To partly answer this question, we applied the BZW procedure to study the electronic properties of GaN, Si, diamond (C), and RuO_2. In what follows, we first describe our method, with emphasis on the BZW procedure. We subsequently present the electronic energy bands, density of states, charge transfer, and related physical properties for gallium nitride. This is followed by our findings for silicon, diamond, and RuO_2. These results are obtained with the optimal basis sets as determined by the BZW procedure. We compare our results to experimental and previous theoretical findings. A discussion of the implications of our work follows. The last section provides a brief conclusion.

II. METHOD

A. General approach: LDA potential and LCAO

The calculations discussed below are nonrelativistic. They are performed at zero temperature. The only effect of temperature that is considered is that obtained by using the applicable lattice parameters. Our calculations utilized an expanded version of the electronic structure calculation program package from the Ames Laboratory of DOE in Iowa.[9–14] Details of the computational method are available in several previous publications.[9–13,2] We employed the Ceperley-Alder type[15] of local-density potentials as parametrized by Vosko, Wilk, and Nusair.[16] The above referenced publications describe the general features of our method, i.e., the LDA potential and the standard implementation of the LCAO. We discuss below our distinctive implementation of the LCGO or LCAO method in a fashion that circumvents the basis set and variational effect noted above.

B. The BZW procedure

In a typical *ab initio*, self-consistent calculation that employs the LCAO method, electronic eigenfunctions are expanded using basis sets derived from atomic calculations.[17,18] Charge densities and potentials are constructed. The Hamiltonian matrix is generated and diagonalized. Key output quantities are energy levels or bands and related wave functions. The resulting output wave functions—for the occupied states—are employed to generate a new charge density and the computations are repeated. The process of using the output of iteration (n)—for occupied states—to construct the input for iteration $(n+1)$ continues until self-consistency is reached. Various measures are utilized to define self-consistency, i.e., when basic quantities, including charge densities, potentials, eigenenergies, etc. are, respectively, unchanged from one iteration to the next.

The trial basis sets are found by various authors by augmenting the atomic orbitals with polarization and diffuse orbitals[17,18] whose numbers, until the work of Bagayoko, Zhao, and Williams[1] and Bagayoko *et al.*,[2] had no particular limit. In fact, from a completeness standpoint, the larger these numbers the better, provided no ‘‘catastrophic sinking of energy levels’’ or negative Millican population numbers occur for occupied states.[17]

The BZW procedure suggests a minimum of three self-consistent calculations that utilize basis sets of different sizes. It generally begins with the minimum basis set, i.e., the basis set needed to account for all the electrons of the atomic or ionic species that are present in a molecule, a cluster, or a solid. In the case of GaN, we chose these species to be Ga^{1+} and N^{1-}. Completely self-consistent calculations are carried out. For the second calculation, the minimal basis set is augmented with one or more atomic orbitals that belong to the next and lowest-lying energy levels in the atomic or ionic species. The self-consistent bands from calculations I and II are compared, graphically and numerically. In general, there will be qualitative (shape and branching) and quantitative (numerical values) differences between the occupied bands from calculations I and II. A third calculation is performed, using the basis set for calculation II as augmented with orbitals representing the next lowest-lying atomic energy levels. This process is continued until the comparison of the occupied energy levels leads to no qualitative or quantitative difference. When the results from calculation N and those from calculation $(N+1)$ agree within the computational error, then the optimum basis set is that of calculation N. This selection rests on the fact that a lowering of unoccupied levels, as in calculation $(N+1)$, after the occupied levels converged with respect to the size of the basis set, as in calculation N, could be a mathematical artifact. Such a lowering may not be the manifestation of any fundamental interaction, but rather the expression of the basis set and variational effect identified above. This assertion is partly verified by computational experiments reported in Sec. III A. In multispecies systems like GaN, two or more orbitals may be added at a time if the affected atomic levels are close in energy. While we utilized the occupied energy bands for the determination of convergence with respect to the size of the basis set, we suspect that other parameters could be employed. They may include the charge density for occupied states and particularly the potential.

C. Computational details

The wurtzite GaN belongs to the C_{6v}^4 group. We considered two sets of lattice parameters for GaN. The low-temperature values we selected are $a=3.16$ Å, $c=5.125$ Å, and $u=0.377$,[3] where u is the distance between the Ga plane and its nearest-neighbor N plane in the unit of c. Even though our calculations are for zero temperature, we also performed calculations for experimentally measured lattice constants for room temperature, where $a=3.1878$ Å, $c=5.1850$ Å, and $u=0.375$.[19] In the C_{6v}^4 group, the Ga and N atoms are in $(2b)$ positions as follows: Ga, (0, 0, 0), (1/3, 2/3, 1/2); N, $(0, 0, u)$, $(1/3, 2/3, 1/2+u)$.

The atomic wave functions of the ionic states of Ga^{1+} and N^{1-} were constructed from the self-consistent, *ab initio* atomic calculations. The radial parts of the atomic wave functions were expanded in terms of Gaussian functions. A set of even tempered Gaussian exponents was employed with a minimum of 0.166 and a maximum of 0.5585×10^5 in atomic unit. We used 19 Gaussian functions for the s and p states and 16 for the d states. A mesh of 24 k points, with proper weights in the irreducible Brillouin zone, was used in the self-consistent iteration calculations. The computational error for the valence charge was about 0.000 22 for 52 electrons. The self-consistent potentials converged to a difference around 10^{-5} after about 35 iterations. The total number of iterations varies with the input potentials.

In the self-consistent LCAO calculations for Si in the diamond structure, we used the experimental lattice constant of $a=5.43$ Å in the calculations. The atomic wave functions were constructed from results of self-consistent, *ab initio* atomic calculations. The radial parts of the atomic wave functions were expanded in terms of Gaussian functions. A set of even-tempered Gaussian exponents was employed with a minimum exponent of 0.099 and a maximum of

TABLE I. The atomic orbitals used in calculations I to V for RuO_2. Superscript zeros indicate added orbitals representing unoccupied atomic levels.

Basis set 0: core-state orbitals in calculations I to V $Ru(1s,2s,3s,2p,3p)$, $O(1s)$
Basis set I: Set 0 plus $Ru(4s,5s,4p,3d,4d)$, $O(2s,2p)$
Basis set II: Set I plus $Ru(5p^0)$, $O(3s^0,3p^0)$
Basis set III: Set II plus $Ru(6s^0)$
Basis set IV: Set III plus $Ru(6p^0)$
Basis Set V: Set IV plus $O(4s^0)$

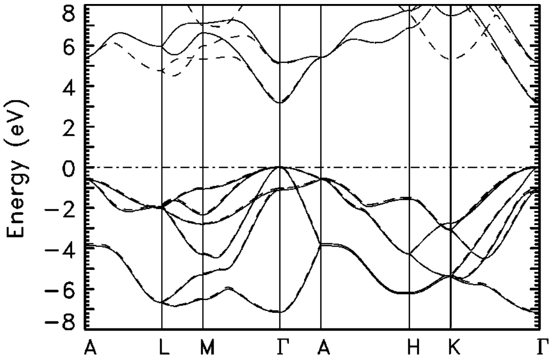

FIG. 1. The calculated, electronic band structure of GaN. The solid lines represent the results of calculation I; the dashed lines show the bands of calculation II. The lattice constants are $a = 3.16$ Å, $c = 5.125$ Å, and $u = 0.377$.

0.65×10^6 in atomic units. We included 19 Gaussian orbitals in the basis set for the expansion of the atomic wave functions of Si. For the extra atomic wave function of $Si(3d^0)$, we used 15 Gaussian orbitals. In the self-consistent calculations, we included 60 general k points in the irreducible Brillouin zone with proper weights. The computational error for the valence charge was about 0.000 95 for 24 electrons. The self-consistent potential converged to about 10^{-5}.

Diamond (C) has a lattice constant of $a = 3.567$ Å. The bond length of the C-C nearest neighbor is 1.545 Å, which is much shorter than the Si-Si bond length of 2.351 Å. The Gaussian functions we used to expand the carbon atomic wave functions have a minimum exponent of 0.12 and a maximum of 0.1×10^6. Sixty k points were used in the self-consistent electronic structure calculations.

Ruthenium dioxide (RuO_2) is a member of the transition-metal oxide family. RuO_2 has a rutile structure and exhibits metallic conductivity. Tetragonal RuO_2 has the symmetry of the $P4_2/mnm(D_{2h}^{14})$ space group.[20] RuO_2 has six atoms per unit cell, two ruthenium and four oxygen. The ruthenium atoms are located at the Wycoff $2(a)$ sites: (0,0,0) and $(\frac{1}{2},\frac{1}{2},\frac{1}{2})$. The oxygen atoms occupy the Wycoff $4(f)$ sites: $\pm(u+\frac{1}{2},\frac{1}{2}-u,\frac{1}{2})$ and $\pm(u,u,0)$. The lattice constants of ruthenium dioxide are $a = 4.492$ Å, $c = 3.106$ Å, and $u = 0.306$.[21] The basis sets for each of the five self-consistent calculations used in the BZW procedure are indicated in Table I. The optimal basis set for the RuO_2 calculation is basis set II in Table I. A total of 25–37 iterations were necessary for convergence. The convergence of the potentials was up to 10^{-5}. We considered 60 k points in the irreducible wedge of the Brillouin zone.

III. RESULTS

A. Electronic energy bands of wurtzite GaN

We have calculated the electronic properties of wurtzite GaN (α-GaN) using the recently introduced procedure.[1,2] Succinctly stated, the implementation of this calculation procedure first consisted of carrying out completely self-consistent calculations for GaN using a minimal LCAO basis set. Namely, the initial charge density for α-GaN was calculated using the atomic orbitals of $Ga(1s2s3s4s, 2p3p4p, 3d)$ and $N(1s2s, 2p)$.

We then repeated the self-consistent calculation using the above basis set as augmented by the orbitals describing the first excited state (i.e., the lowest in energy) of Ga. Hence, $Ga(4d^0)$ orbitals were added to the basis set. The superscript index of zero indicates that these states are unoccupied in the free atoms (ions). We then plotted the energy bands obtained from these two distinct self-consistent calculations. In Fig. 1 the solid and dashed lines represent the calculated results from the first and second calculations, respectively. Figure 1 shows that the occupied bands from the two calculations differ slightly. In particular, the difference is not a rigid shift of one set of bands with respect to the other. Hence, as noted above, the larger basis set, for the second self-consistent calculation, is preferred to that for the first. This preference is based on physical considerations, i.e., actual, physical interactions are responsible for the difference between the two sets of bands. Completeness requirements, partly to describe the redistribution of the electronic cloud in the solid environment, dictate this preference. The next natural step was to repeat our procedure, for a third time, with a new basis set that includes a $N(3s^0)$ orbital. The results of this third calculation (dashed lines) and of the second calculation (solid lines) are shown in Fig. 2. Unlike in the case of Fig. 1, the calculated bands for occupied states are fully converged. In particular, the changes in occupied energies, from calculation II to III, are in the range of computational errors that are due to other factors, including rounding errors and possible limitations of LDA. In contrast to the unchanged nature of the occupied states, the lowest unoccupied states at the Γ and A symmetry points are shifted downward by approximately 0.8 eV.

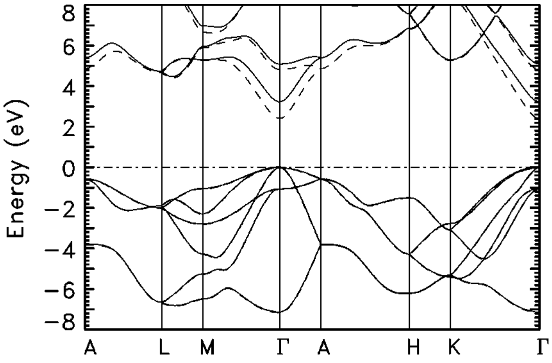

FIG. 2. Comparison of the results of calculation II and III. The solid lines represent the GaN electron bands from calculation II; the dashed lines show the bands from calculation III. The lattice constants are $a = 3.16$ Å, $c = 5.125$ Å, and $u = 0.377$.

TABLE II. The calculated electronic energy levels (in eV) for wurtzite GaN using two sets of lattice constants. Calculation A (LDA A): $a=3.160$ Å, $c=5.125$ Å, and $u=0.377$. Calculation B (LDA B): $a=3.1878$ Å, $c=5.1850$ Å, and $u=0.375$. The lattice constants in the *GW* calculations of Rubio *et al.* are those for calculation A. The minimum band gaps are the energies at Γ_{1c}. See our theoretical DOS for the calculated, low-temperature, ‘‘practical’’ band gap of 3.4 eV.

GaN	LDA A	LDA B	Rubio LDA	Rubio *GW*		LDA A	LDA B	Rubio LDA	Rubio *GW*
Γ_{3v}	−7.1	−7.0	−7.4	−8.0	M_{1v}	−6.5	−6.3	−6.8	−7.4
Γ_{5v}	−1.1	−1.0	−1.1	−1.2	M_{3v}	−5.3	−5.1	−5.6	−6.1
Γ_{5v}	−1.1	−1.0	−1.1	−1.2	M_{1v}	−4.3	−4.2	−4.4	−4.9
Γ_{1v}	0.0	0.0	0.0	0.0	M_{2v}	−2.8	−2.7	−2.8	−3.1
Γ_{6v}	0.0	0.0	0.0	0.0	M_{3v}	−2.3	−2.2	−2.4	−2.6
Γ_{6v}	0.0	0.0	0.0	0.0	M_{4v}	−1.1	−1.0	−1.0	−1.1
Γ_{1c}	3.2	3.0	2.3	3.5	M_{1c}	5.3	5.3	5.1	6.5
Γ_{3c}	5.1	4.9	4.6	5.9	M_{3c}	5.9	5.8	5.7	7.4
Γ_{6c}	10.2	10.1	10.1	11.9	M_{3c}	7.0	6.7	6.2	8.1
Γ_{1c}	10.3	10.1	9.5	12.1	M_{1c}	9.3	9.1	9.1	11.5
$A_{1,3v}$	−3.8	−3.8	−4.1	−4.6	$L_{1,3v}$	−6.7	−6.5	−7.0	−7.6
$A_{5,6v}$	−0.6	−0.5	−0.5	−0.6	$L_{2,4v}$	−2.0	−1.9	−2.0	−2.2
$A_{5,6v}$	−0.6	−0.5	−0.5	−0.6	$L_{1,3v}$	−1.9	−1.9	−2.0	−2.2
$A_{1,3c}$	5.4	5.2	4.6	6.1	$L_{1,3c}$	4.7	4.6	4.4	6.0
$A_{5,6c}$	9.2	9.0	8.7	10.8	$L_{1,3c}$	8.3	8.1	8.0	9.9
K_{1v}	−5.4	−5.2	−5.6	−6.1	H_{3v}	−6.2	−6.1	−6.4	−7.1
K_{3v}	−5.3	−5.2	−5.5	−6.1	$H_{1,2v}$	−4.3	−4.1	−4.6	−4.9
K_{3v}	−3.1	−3.0	−3.2	−3.5	H_{3v}	−1.5	−1.5	−1.5	−1.6
K_{2v}	−2.8	−2.6	−3.0	−3.2	H_{3c}	6.8	6.7	6.6	8.3
K_{2c}	5.3	5.3	4.9	6.6	$H_{1,2c}$	7.5	7.4	7.4	9.4
K_{3c}	8.6	8.4	8.3	10.6					

In light of the iteration procedure described above, and that only includes the wave functions of occupied states in the reconstruction of the charge density, potential, and Hamiltonian, the preferred basis set is that in calculation II. The drastic changes in the unoccupied states, in going from calculation II to III, are believed to be simple consequences of the variational theorem noted above. Namely, this lowering may not be due to a physical interaction, but rather to a mathematical artifact stemming from the variational theorem. While no other graphs are shown here, we continued to add orbitals of higher and higher excited states to the basis set for calculation four and five. As expected, these calculations did not lead to changes in the occupied states. They led, expectedly, to drastic changes in higher and higher, unoccupied bands.

Our claim relative to the use of the wave functions of the occupied states in the self-consistent procedure as a basis for preferring the optimum basis set to larger ones is verified by the following computational experiments. These computational tests, on GaN, addressed the self-consistency of the potential and the effect of the size of the basis set separately. We diagonalized the Hamiltonian matrix, using the larger basis set of calculation III, while utilizing only the self-consistent potential obtained with the optimum basis set. The bands resulting from this diagonalization—for both the occupied and unoccupied states—are the same as the dashed lines in Fig. 2. We also utilized the self-consistent potential obtained with the optimum basis set and diagonalized the Hamiltonian using the minimum basis set. The bands from this calculation closely follow those of calculation II for the occupied states and those of calculation I for the unoccupied states. These tests verified that the potential obtained with the optimum basis is practically identical to that generated with the larger basis set of calculation III and that it is different from the potential obtained with a basis set smaller than the optimum one. A comparison of the results of the diagonalization tests noted above to the self-consistent bands obtained with the optimum basis set is revealing. It consists of a comparison of the effects of the size of the basis set, given that all three calculations employed the self-consistent potential obtained in calculation II. A plot of the results of the diagonalization, using the basis set of calculation III and the self-consistent potential from calculation II, and of the bands from calculations II practically reproduces Fig. 2. Similarly, Fig. 1 is practically obtained by graphing the results of calculation II and those of the diagonalization using the basis set in calculation I and the self-consistent potential from calculation II. These computational experiments verified our contention that due to the variational theorem and the use of the wave functions of the occupied states only in the iterative procedure, the optimum basis set as defined above should be selected instead smaller or larger basis sets.

The electronic band structure of α-GaN, obtained with the optimum basis set of calculation II, is shown in Fig. 2 in solid lines. The zero of the energy is set at the top of the valence band. In our nonrelativistic calculations, the effect of spin-orbit interaction is not considered.

Table II lists the energy levels at high symmetry points in the Brillouin zone for both sets of lattice constants. It also shows, for the same points, the LDA and GW results of Rubio *et al.*[3] Our results in columns two and seven (calculation A) are the ones to compare with the GW findings of Rubio *et al.*, as they are obtained with the same low-temperature lattice constants specified in Table II. The LDA results of Rubio *et al.* were obtained at slightly different lattice constants representing their theoretical LDA values ($a=3.126$ Å, $c=5.119$ Å, $u=0.377$). Our results in columns three and eight were obtained for room-temperature values of the lattice parameters (calculation B).

Our LDA results from calculation A are different from the LDA findings of Rubio *et al.*, particularly for the conduction bands. Some of these differences are due to that between the sets of lattice constants. Upon superposing the tops of the valence bands, their LDA bands are systematically lower than or the same as ours in energy, except at M_{4v} and $A_{5,6v}$. Their GW results are systematically lower and higher than ours for the occupied and unoccupied states, respectively. In all cases, our calculated conduction bands for low temperature lie between their corresponding LDA and GW results. As expected from the band structure in Fig. 2, the differences between their LDA results and ours are the smallest at the H and L symmetry points. The least lowering of unoccupied levels occurs at these points, when basis sets larger than the optimal one are utilized.

The largest difference between corresponding LDA energies for the occupied states is 0.3 eV. This is also the largest difference between occupied or unoccupied LDA energies at the H and L points. In contrast to the case of occupied states, some LDA conduction-band energies, from the work of Rubio *et al.*, are up to 0.9 eV (at Γ_{1c}) lower than that of our corresponding values. Except at Γ_{1c} where the difference is just 0.3 eV in magnitude, the GW results for the conduction bands are generally 0.7 to 2.2 eV higher in energy than we found in calculation A (LDA with low-temperature lattice constants). For the lowest valence states in Table II, the GW results are 0.7 (at K_{1v}) to 1.1 eV (at $L_{1,3v}$) lower than our LDA findings.

The effective mass is a measure of the quality of the calculated bands. Specially, the agreement between calculated and measured effective masses indicates an accurate determination of the shape of the bands. Our calculated effective mass for the n-type carriers of α-GaN near the Γ point is $0.22\pm0.03m_0$. This result is in a good agreement with the experimental data of $0.2\pm0.02m_0$.[22,23]

B. Density of states, band gap, and charge distribution for GaN

Figures 3 and 4, respectively, show the total and partial density of states (DOS) for wurtzite GaN, as obtained from calculation A. While much difference is not expected between our DOS and those obtained from previous LDA calculations, for the occupied states, significant discrepancies are obvious for the unoccupied levels. In particular, previous LDA calculations, on account of results in Fig. 2 and Table II, have conduction-band DOS that are shifted toward lower energies as compared to ours. This shift, as per Fig. 2, is not rigid. On the other hand, the GW results of Rubio *et al.*, for the conduction bands, are shifted toward much higher energies as compared to ours.

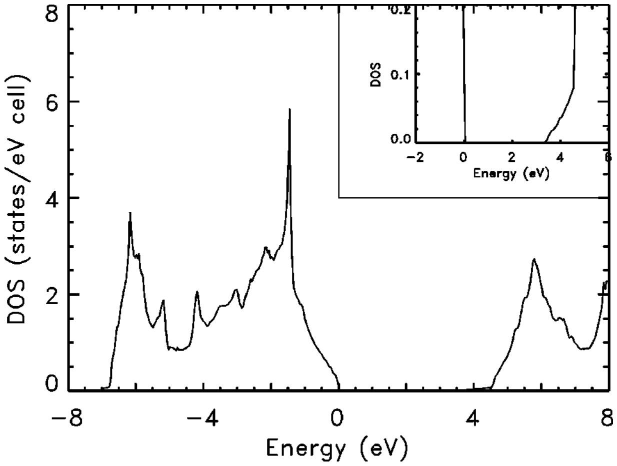

FIG. 3. The calculated density of states for wurtzite GaN, as obtained from the bands in solid lines in Fig. 2. The inset shows that the practically measurable band gap is 3.4 eV.

The band gap, until now, has been generally calculated as the difference between the energies for the minimum of the conduction band and the maximum of the valence band. We refer to this band gap, calculated in this fashion, as the theoretical, ''minimum'' band gap. Our calculation A, with low-temperature lattice parameters, found a minimum gap of 3.2 eV, while the LDA and GW works of Rubio *et al.*, respectively, reported 2.3 and 3.5 eV. These minimum band gaps are the energies at Γ_{1c} in Table II. These gaps, as per Table II or Fig. 2, are direct gaps found at the Γ point. Our total DOS curve in Fig. 3, particularly the inset, shows that the calculated, ''practical,'' and measurable band gap for low-temperature GaN is 3.4 eV–in excellent agreement with experiment.[23–26] Indeed, the specially parabolic feature of the bands around Γ_{1c} leads to the very small tail structure that is likely to be difficult to measure. The reported experi-

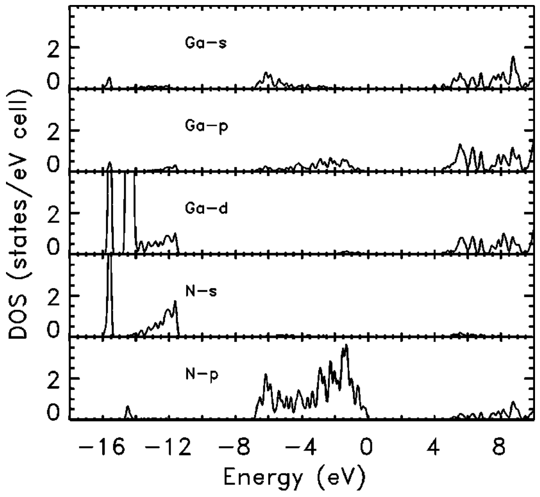

FIG. 4. The PDOS for wurtzite GaN from the contribution of the s, p, and d states of Ga atoms and from the s and p states of N atoms. These PDOS are derived from the bands (solid lines in Fig. 2) obtained with the BZW optimal basis set.

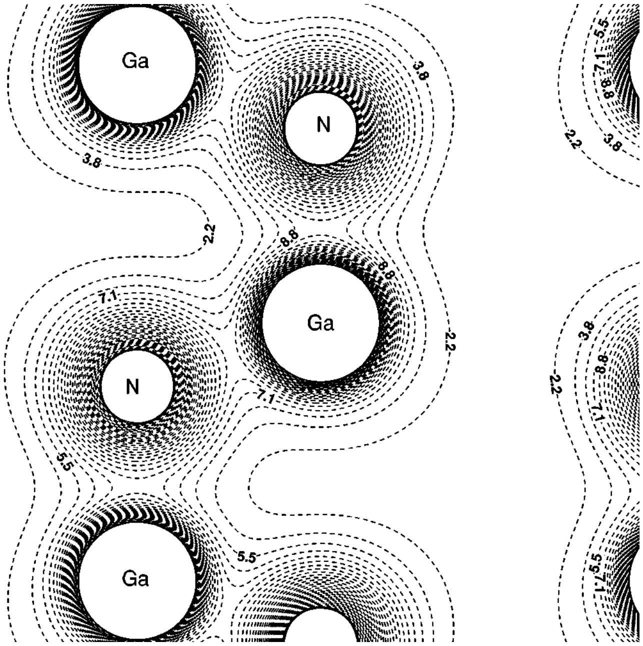

FIG. 5. The charge density distribution on a (010) plane passing through Ga and N atoms. The lattice constants (room temperature) are $a = 3.1878$ Å, $c = 5.1850$ Å, and $u = 0.375$.

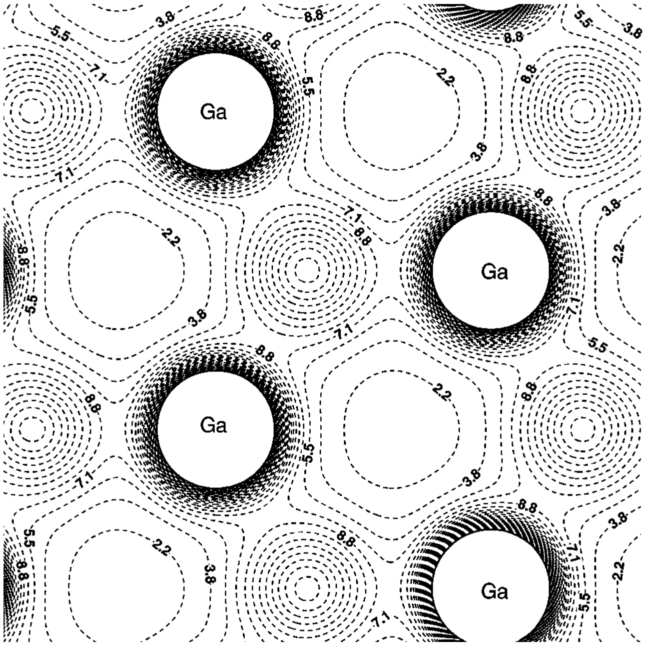

FIG. 6. The charge density distribution on a (001) plane of Ga atoms. The lattice constants (room temperature) are $a = 3.1878$ Å, $c = 5.1850$ Å, and $u = 0.375$.

mental optical-absorption spectrum[25] actually shows the need to define a ''practical'' band gap, distinct from the minimum band gap. The GW minimum gap of 3.5 eV is therefore expected to lead to a measurable band gap of approximately 3.7 eV or higher, assuming that the GW bands preserved the parabolic structure around Γ_{1c}. Our calculation B, with room-temperature lattice constants specified in Table II, found a minimum band gap of 3.0 eV and a practical band gap of 3.2 eV, in excellent agreement with room-temperature experiment.[23,26]

We also calculated the effective charge and charge transfer for wurtzite GaN using the obtained electron wave functions. The calculated charge transfer led to an effective ionic formula of $\mathrm{Ga}^{1.5+}\mathrm{N}^{1.5-}$ for wurtzite gallium nitride.

Figures 5 and 6 show the contour plots of the charge distribution, for room-temperature lattice constants (calculation B), in different symmetry planes, i.e., a (010) plane containing Ga and N atoms, and a (001) plane containing Ga atoms. The unit of the labeled charge density values is 10^{-2} electrons/a_0^3, where $a_0 = 0.529\,177$ Å. The high charge-density region around the nuclear sites has been cut off in these diagrams at a value of 0.5 electrons/a_0^3, leaving hollow spheres to represent the atomic cores. There are some portions of empty space in the wurtzite structure of GaN, as seen from the charge distribution in Figs. 5 and 6. The empty tubes are distributed in a hexagonal structure along the c direction. The calculated electron charge distribution of Fig. 5 indicates that there is a quite strong covalent character of the Ga-N bonds. This can be seen from the noticeable charge distribution at the middle of the Ga-N bond. The size of the nitrogen ions appears larger than that of gallium ions in Fig. 5. The radii of the Ga and N ions in wurtzite GaN are estimated as $r(\mathrm{Ga}) = 0.92$ Å and $r(\mathrm{N}) = 1.01$ Å.

C. Electronic properties and optical transitions in silicon

Silicon is probably the best known semiconductor. It has been studied for more than 40 years. We found that the *optimum basis set* for the LCAO calculation consists of the atomic orbitals of $\mathrm{Si}(1s2s3s4s\,2p3p\,3d)$. Here, the $\mathrm{Si}(4s\,3d)$ are empty shells and are used to augment the basis set to account for charge redistributions in the solid environment. The electron band structure of Si, calculated with the optimum basis set, is shown in Fig. 7 without spin-orbit interaction. Figure 7 shows that the top of the valence band is at the Γ point. The minimum of the conduction band is at a general point between Γ and X. The calculated indirect band gap is about 1.02 eV, which is very close to the experimental value of about 1.14–1.17 eV.[27,28] The calculated conduction band minima are at $(2\pi/a)(0.79,0,0)$ and at the equivalent points, one along each cube edge. The effective mass of the n-type carriers at the conduction-band minimum is very anisotropic. The calculated transverse and longitudinal effective masses are, from the band dispersions in Fig. 7, $m_{nt} = 0.20 \pm 0.03 m_0$ and $m_{nl} = 0.93 \pm 0.03 m_0$, respectively.

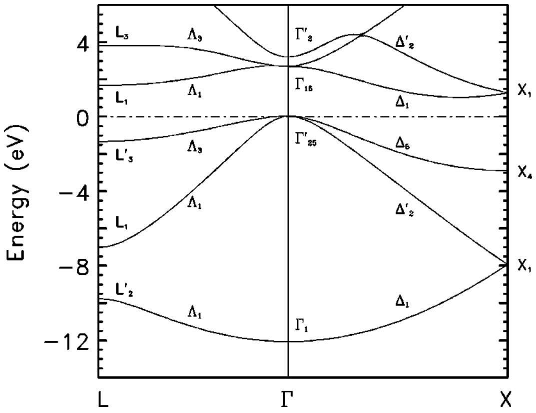

FIG. 7. The calculated electron band structure of Si along the symmetry directions Λ and Δ, as obtained with the optimal basis set of the BZW procedure.

TABLE III. Comparison of the calculated interband-transition energies (in eV) for silicon (Si) with experimental results.

Si	This calculation	Measurements
E_g	1.02	1.14,[a] 1.17[b]
$\Gamma_{1v}\rightarrow\Gamma'_{25v}$	12.1	12.5 ± 0.6[b]
$\Gamma'_{25v}\rightarrow\Gamma_{15c}$	2.68	3.0,[c] 3.4[d]
$\Gamma'_{25v}\rightarrow\Gamma'_{2c}$	3.19	
$X_{4v}\rightarrow\Gamma'_{25v}$	2.93	2.9,[e] 3.3 ± 0.2[f]
$\Gamma'_{25v}\rightarrow X_{1c}$	1.26	1.3[b]
$L'_{2v}\rightarrow\Gamma'_{25v}$	9.80	9.3 ± 0.4[b]
$L_{1v}\rightarrow\Gamma'_{25v}$	7.04	6.8 ± 0.2[b]
$L'_{3v}\rightarrow\Gamma'_{25v}$	1.36	1.2 ± 0.2[b]
$\Gamma'_{25v}\rightarrow L_{1c}$	1.66	1.65,[g] 2.1[h]
$\Gamma'_{25v}\rightarrow L_{3c}$	3.78	3.9 ± 0.1,[b] 4.15 ± 0.01[i]
$L'_{3v}\rightarrow L_{1c}$	3.0	3.2 ± 0.2,[b] 3.45[d]
$L'_{3v}\rightarrow L_{3c}$	5.14	5.1 ± 0.2,[b] 5.5[d]

[a] Reference 27.
[b] Reference 28.
[c] Reference 29.
[d] Reference 30.
[e] Reference 31.
[f] Reference 32.
[g] Reference 33.
[h] Reference 34.
[i] Reference 35.

These calculated effective masses are very close to the experimental values of $m_{nt}=0.19m_0$ and $m_{nl}=0.98m_0$.[28] The good agreements between the calculated effective mass and the band gap, with corresponding experimental results, indicate that the lowest conduction band in Fig. 7 is reasonably reliable.

Table III shows the calculated interband-transition energies, along with experimental results, at selected critical points in the optical spectrum. In this table the indices v and c refer to the valence and conduction bands, respectively. The calculated optical transitions agree well with experimental results. This agreement is particularly significant in light of difficulties in analyzing experimental data, including the effect of lifetime corrections. These corrections are expected to be significant for larger transition energies. In the experimental optical spectrum, each of the structures includes all possible optical transitions. The assignment of one structure to a particular transition from the experimentally measured optical spectrum has been a difficult problem in solid-state spectroscopy.[36] The reported experimental $\Gamma'_{25v}\rightarrow\Gamma'_{2c}$ transition energy of 4.2 eV from the low-field electron-reflectance measurement,[36] disagree with the calculated value of 3.19 eV. Our calculated data suggest that the 4.2 eV transition is rather the $X_{4v}\rightarrow X_{1c}$ transition energy. This conjecture is based on the following reasons. (1) The small phase-space volume around the Γ'_{2c} point only contribute a tail-like structure to the density of states and to the optical spectrum. (2) The Δ_5 and Δ_1 bands are nearly parallel for a substantial portion of the phase-space volume, increasing the possibility for mistaken assignment of structures, and the calculated transition energies from X_{4v} to X_{1c} states are about 4.2 eV. (3) The doubly degenerate Δ_5 bands have a spin-orbit splitting from the Γ'_{25} to the X_4 points, consistent with the experimental observations of the peak structures.

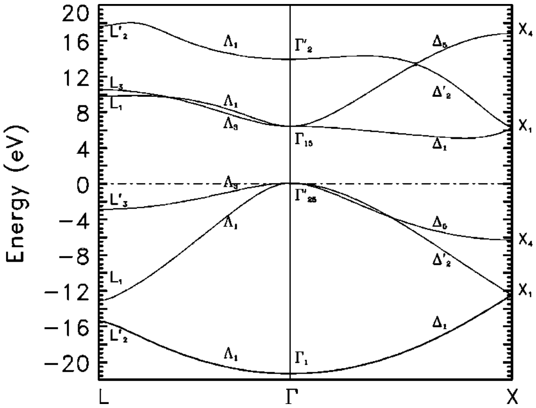

FIG. 8. The calculated electron band structure of diamond (C) along the symmetry directions Λ and Δ, as obtained with the optimal basis set of the BZW procedure.

The $\Gamma_{1v}\rightarrow\Gamma'_{25v}$ transition is a measure of the valence-band width. Our calculated valence-band width of 12.1 eV is in an excellent agreement with the experimentally measured value of 12.5 ± 0.6 eV.

D. Electronic properties and optical transitions of diamond

The BZW procedure leads to an optimum basis set of $C(1s2s3s\,2p)$ for the LCAO calculation for diamond. Here, the $C(3s)$ orbital is empty. The calculated electronic band structure of diamond is shown in Fig. 8. The top of the valence band (band edge) is at the Γ point. The bottom of the conduction band is near $(2\pi/a)(0.81,0,0)$. The calculated indirect band gap (E_g) is about 5.05 eV, which is close to the experimental value of about 5.3–5.48 eV.[27,28] There are some experimental complications in determining the exact band gap, including the tails of the optical spectra that can extend to several tenths of an eV.[37,38] The calculated effective masses for the n-type carriers around the conduction-band edge are $m_{n\parallel}=1.1\pm0.2m_0$ and $m_{n\perp}=0.30\pm0.03m_0$. Here, the notations $\parallel$ and $\perp$ refer to the directions parallel and perpendicular to the Δ_1 band, respectively. Our calculated effective masses are very close to the reported experimental results of $m_{n\parallel}=1.4m_0$ and $m_{n\perp}=0.36m_0$.[28] There is a strong nonparabolic dispersion of the Δ_1 band around the conduction-band minimum. This leads to a relatively larger uncertainty in obtaining the effective mass and is also part of the reason for the differences in calculations of the effective masses for $m_{n\parallel}$, using different methods.

We listed in Table IV some calculated interband-transition energies at selected critical points. The calculated valence-band width of 21.35 eV is in an excellent agreement with the experimental value of 21 ± 1 eV. The calculated transition energies agree very well with experimental results.

E. Electronic properties of RuO_2: Negligible BZW corrections for metals

Our results for the calculated electronic band and related wave functions are characterized by the following two major points: (a) our calculations II through V gave exactly the same results for the valence and low-lying conduction bands

TABLE IV. The calculated interband-transition energies (in eV) for diamond (C).

Diamond	This calculation	Measurements
E_g	5.05	5.3,[a] 5.48[b]
$\Gamma_{1v}\rightarrow\Gamma'_{25v}$	21.35	21 ± 1,[c] 24.2 ± 1[d]
$\Gamma'_{25v}\rightarrow\Gamma_{15c}$	6.36	6.0 ± 0.2,[b] 7.3[e]
$\Gamma'_{25v}\rightarrow\Gamma'_{2c}$	13.87	15.3 ± 0.5[f]
$L'_{2v}\rightarrow\Gamma'_{25v}$	15.49	15.2 ± 0.3[f]
$L_{1v}\rightarrow\Gamma'_{25v}$	13.18	12.8 ± 0.3[f]

[a] Reference 27.
[b] Reference 28.
[c] Reference 37.
[d] Reference 39.
[e] Reference 38.
[f] Reference 37.

in Fig. 9, and (b) these results almost perfectly reproduce those of Ref. 40. The significance of these points stems from the fact that they clearly indicate that corrections expected from the application of the BZW procedure are negligible for metallic RuO_2, unlike in the case of semiconductors. Consequently, our calculated total density of states (DOS) in Fig. 10 are the same as those of Glassford and Chelikowsky[40]—in qualitative and quantitative terms. These authors did not provide the partial density of states (PDOS) we show in Fig. 11. These PDOS qualitatively agree with some results of Schwarz.[41] Our PDOS are different from those obtained by Schwarz for energies between -5 and -10 eV. The differences are both qualitative and quantitative. For instance, our calculated PDOS for Ru 4*d* and O 2*p* clearly show a double-peak structure not discernible from the augmented spherical wave (ASW) results of Schwarz. The magnitudes of the peaks in Fig. 11, between -5 and -10 eV, are more than double the corresponding ones as obtained by Schwarz. We ascribe these discrepancies to differences between our *ab initio* calculations and the ASW method.

The negligible nature of the BZW corrections for metallic RuO_2, as illustrated above, pertains only to descriptive calculations. Namely, computations of properties of a material known to be a metal at a given stoichiometric composition and under specified conditions of temperature and pressure. The BZW procedure is expected to be necessary for predictive calculations, i.e., those for materials whose metallic state is not known or for which elemental composition and related concentrations, pressure, or temperature are changed. While no discrepancies were found between our calculations II to V, for the valence and low-energy conduction bands, the variational theorem necessarily leads to differences for the highest conduction bands. For instance, the fundamental theorem of algebra dictates that the number of calculated eigenenergies increase as the size of the Hamiltonian increases.

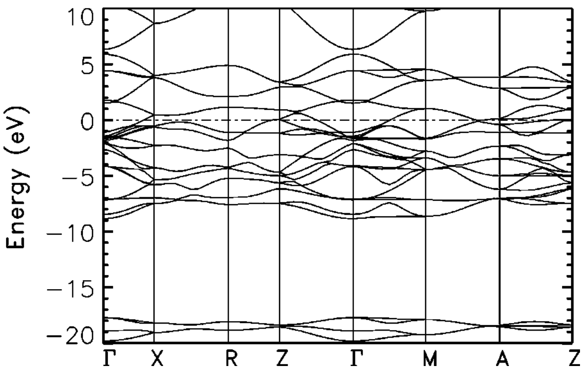

FIG. 9. The electronic band structure of RuO_2 obtained with the BZW optimal basis set. All results here were obtained with basis set II. The shown bands are the same for calculations III–V.

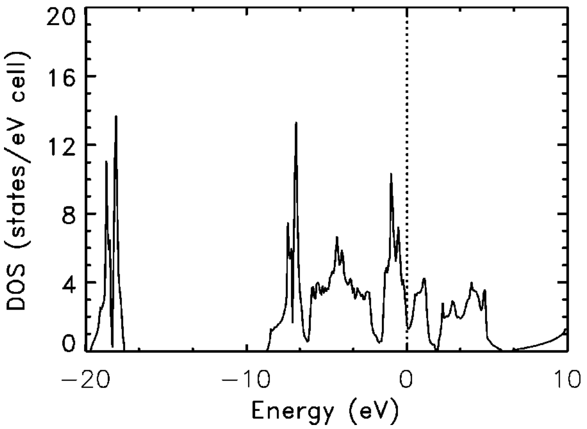

FIG. 10. The DOS for RuO_2.

IV. DISCUSSION

A. Choices of basis sets and of lattice parameters

It is important to note that the optimal size of the basis set for a given calculation varies with the nature and quality of the trial orbitals. Two computations for the same material, using Gaussian orbitals, are expected to lead to different sizes of the optimal basis set if the Gaussian exponents in the two calculations are different. The essential point is that both calculations must properly implement the procedure to arrive at the optimal size that applies, given the input orbitals. Fur-

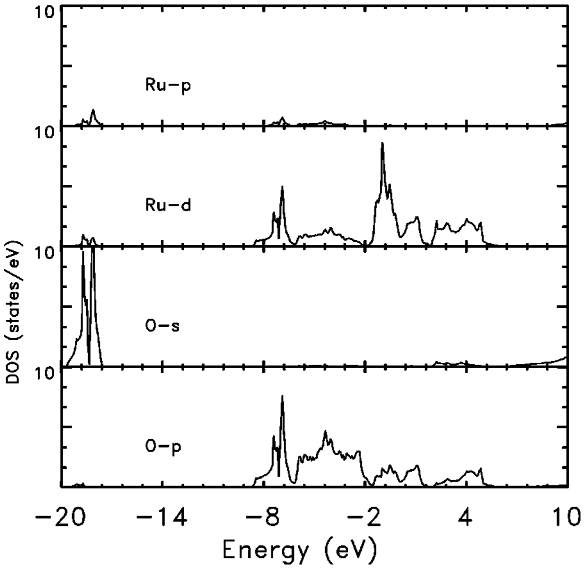

FIG. 11. The PDOS for RuO_2.

ther, Bagayoko showed[18] that the use of contraction of orbitals leads to a rigid shift of the bands. This rigid shift does not affect the physics of the problem. It is a simple manifestation of the referenced variational theorem. The bands obtained with contracted orbitals are shifted upwards as compared to those obtained with uncontracted orbitals—where the dimension of the matrices in the eigenvalue problem is larger.

The above points apply irrespective of the nature of the trial orbitals, i.e., Gaussian, exponential, or others, provided the increases in the size of the basis set progressively account for higher and higher energy orbitals of the input species (atoms or ions). In the case of plane waves, and in light of the relatively large number of orbitals, the implementation of the BZW procedure is expected to be more time consuming if plane waves are added or subtracted one at a time. Additionally, complications arise if higher and higher exponent plane waves are added, as done in some plane-wave calculations, as opposed to beginning with the highest exponents (representing lower, occupied states). The difficulties could be reduced by using augmented plane waves. The adequacy of the trial basis set directly affects the number of additions or subtractions of orbitals for the purpose of determining the optimal basis set for molecules, clusters, or solids. As in the case of Gaussian orbitals, a set of the trial functions describing the ground states of the affected atomic or ionic species is expected to be a good start.

Our choices for the lattice constants were dictated by two considerations. The first one stems from the fact that our program package does not yet include accurate codes for the calculation of the total energy. The search for equilibrium lattice parameters requires high accuracy. The second consideration, equally important, actually dictates that we utilize experimental lattice constants for some comparisons with measurements to be meaningful. Specifically, in the case of GaN, we considered two sets of lattice parameters to enable general comparison with experimental findings and specific comparison with the low-temperature results of Rubio *et al.* In the case of silicon and diamond, matters are complicated further by the fact that some experiments reported slightly different lattice constants. While the use of experimental lattice parameters, as opposed to those for the minimum of the total energy curve versus the lattice parameter, is tantamount to applying pressure to a solid, the results discussed here are best fit for comparison with actual measurements.

B. LDA prediction of properties of semiconductors

The comparison of our results for GaN with those of the *GW* work of Rubio *et al.*[3] should be placed in context. Namely, their *GW* results were obtained by utilizing the valence state eigenfunctions of their LDA calculations. Specifically, their Eq. (3) (Ref. 3) is $E_{n\mathbf{k}}=\epsilon_{n\mathbf{k}}^{LDA}+\langle n\mathbf{k}|\Sigma(E_{n\mathbf{k}})-V_{xc}^{LDA}|n\mathbf{k}\rangle$, where $E_{n\mathbf{k}}$ is the *GW* quasiparticle energy, $\epsilon_{n\mathbf{k}}^{LDA}$ is the corresponding LDA eigenvalue, and $\Sigma(E_{n\mathbf{k}})$ is the energy-dependent self-energy. V_{xc}^{LDA} is the LDA exchange-correlation potential, and $|n\mathbf{k}\rangle$ is the LDA wave function at **k** for band n. In the above equation, $\epsilon_{n\mathbf{k}}^{LDA}$ is increased or decreased by the many-body correction. The differences between our results and the non-ground-state, quasiparticle eigenenergies from the *GW* calculations are due not only to the difference between the states of the system under considerations, but also to the difference between our LDA results and those of Rubio *et al.*[3] The *GW* eigenenergies are not for the ground state of GaN, as in the case for LDA. They rather belong to a GaN many-body system to or from which an electron is added or removed,[42] respectively. We conjecture that the above corrections could be small if LDA results do not include the basis set and variational effect for some unoccupied bands.

Our results, as presented above, clearly established that some limitations previously ascribed to local-density approximation are not necessarily due to LDA. In particular, and as far as GaN is concerned, a basis set and variational effect was confounded with limitations, if any, of LDA. Bagayoko *et al.* showed the above assertion to hold for their LDA description of $BaTiO_3$.[2]

The possible overestimate of the band gap by quasiparticle calculations is not unique for GaN. The results of Hybertsen and Louie[42] for Si and those of Rohlfing, Krüger, and Pollmann[43] for Si and C are consistently above the experimental numbers. Schöne and Eguiluz[44] recently performed self-consistent *GW* calculations for silicon. They reported a minimum (or absolute) self-consistent band gap of 1.91 eV for silicon. The non-self-consistent gap was 1.34 eV. These authors assert that the self-consistent *GW* overestimates the band gap by as much as ''previous'' LDA underestimated it. The point of our work, we hope, is to show that the BZW procedure, by avoiding the basis set and variational effect noted above, clearly predict the low, unoccupied energy levels or bands and the band gap—within a local-density approximation.

These results raise questions about other disagreements between LDA and experimental findings. Specifically, the universality of the basis set and variational effect indicates that the BZW procedure should give improved LDA results for molecules, clusters, semiconductors, and insulators. The work of Williams[6] suggests that in the case of metals, the basis set and variational effect should generally be very small. This situation is intuitively understandable in light of the crossing of the Fermi level by some bands. The occupied bands and several low-lying conduction bands converge, simultaneously, with respect to the size of the basis set. This situation partly explains the relative success of previous LDA calculations in describing metals[45] as compared to semiconductors or insulators.

This work and related ones[2,6] noted above established the predictive capability of LDA—provided the BZW procedure is utilized. This procedure avoids the basis set and variational effect on unoccupied eigenstate energies in molecules, clusters, semiconductors, and insulators, while ensuring adequate completeness of the basis set as measured by the convergence of the physical quantities with respect to the size of the basis set. Future calculations with the BZW procedure, we contend, are expected to show a similar predictive capability for other computations based on density-functional theory,[46,47] including investigations using fully relativistic,[48] nonlocal,[49] or temperature-dependent[48] potentials. The applications of the procedure are not limited to density-functional calculations. The BZW procedure is expected to be needed in many self-consistent calculations that utilize basis sets and reconstruct intermediate quantities (i.e., charge density), using only some attributes (i.e., wave functions) of the occupied states.

V. CONCLUSION

Our calculated LDA valence-band structures of GaN, Si, and diamond (C) generally agree with those from previous first-principle calculations. Moreover, our calculated, low-energy conduction bands, band gaps, and effective masses of *n*-type carriers also agree well with experimental results. This work and the related ones noted above established a predictive capability for the local-density approximation in describing properties of materials. Further, the BZW procedure is expected to be needed by most self-consistent calculations utilizing basis sets in a variational method of the Rayleigh-Ritz type—as long as intermediate steps utilize the wave functions of the occupied states only.

ACKNOWLEDGMENTS

This work was supported in part by funding from the U.S. Department of the Navy, Office of Naval Research (ONR), through the Timbuktu Academy (Grants No. N00014-93-1-1368 and No. N00014-98-1-0748), from the graduate program in the Department of Physics, Southern University and A & M College, and from the Louisiana Board of Regents' Support Fund [Contracts No. LEQSF (1996-1997)-ENH-TR-55 and No. LEQSF (1994-98)-GF-18].

---

[1] D. Bagayoko, G. L. Zhao, and T. D. Williams, Bull. Am. Phys. Soc. **43**, 846 (1998).

[2] D. Bagayoko, G. L. Zhao, J. D. Fan, and J. T. Wang, J. Phys.: Condens. Matter **10**, 5645 (1998).

[3] A. Rubio, J. L. Corkill, M. L. Cohen, E. L. Shirley, and S. G. Louie, Phys. Rev. B **48**, 11810 (1993).

[4] D. Vogel, P. Krüger, and J. Pollmann, Phys. Rev. B **55**, 12 836 (1997).

[5] J. Perdew and A. Zunger, Phys. Rev. B **23**, 5048 (1981).

[6] T. D. Williams, M.S. thesis, Southern University and A & M College, Baton Rouge, 1998.

[7] S. H. Gould, *Variational Methods for Eigenvalue Problems* (University of Toronto Press, Toronto, 1957), Chap. 2.

[8] S. G. Mikhlin, *The Numerical Performance of Variational Methods* (Wolters-Noordhoff, Groningen, 1971), Chaps. 1, 2, and 7.

[9] W. Y. Ching, J. Am. Ceram. Soc. **73**, 3135 (1990).

[10] P. J. Feibelman, J. A. Appelbaum, and D. R. Hamann, Phys. Rev. B **20**, 1433 (1979).

[11] B. N. Harmon, W. Weber, and D. R. Hamann, Phys. Rev. B **25**, 1109 (1982).

[12] G. L. Zhao, T. C. Leung, B. N. Harmon, M. Keil, M. Muller, and W. Weber, Phys. Rev. B **40**, 7999 (1989).

[13] G. L. Zhao and B. N. Harmon, Phys. Rev. B **45**, 2818 (1992).

[14] W. Y. Ching, Y. Xu, G. L. Zhao, K. W. Wong, and F. Zandiehnadem, Phys. Rev. Lett. **59**, 1333 (1987).

[15] D. M. Ceperley and B. J. Alder, Phys. Rev. Lett. **45**, 566 (1980).

[16] S. H. Vosko, L. Wilk, and M. Nusair, Can. J. Phys. **58**, 1200 (1980).

[17] D. Bagayoko, P. M. Lam, N. Brener, and J. Callaway, Phys. Rev. B **54**, 12 184 (1996).

[18] D. Bagayoko, Int. J. Quantum Chem., Quantum Chem. Symp. **17**, 527 (1983).

[19] M. Leszczynski, H. Teisseyre, I. Suski, I. Grzegory, M. Bockowski, J. Jun, S. Porowski, K. Pakula, J. M. Baranowski, C. T. Foxon, and T. S. Cheng, Appl. Phys. Lett. **69**, 73 (1996).

[20] D. B. Rogers, R. D. Shannon, A. W. Sleight, and J. L. Gillson, Inorg. Chem. **8**, 841 (1969).

[21] J. H. Xu, T. Jarlborg, and A. J. Freeman, Phys. Rev. B **40**, 7939 (1989).

[22] W. J. Moore, J. A. Freitas, and R. J. Molnar, Phys. Rev. B **56**, 12 073 (1997).

[23] S. Strite and H. Morkoc, J. Vac. Sci. Technol. B **10**, 1237 (1992).

[24] M. O. Manasreh, Phys. Rev. B **53**, 16 425 (1996).

[25] H. P. Maruska and J. J. Tietjen, Appl. Phys. Lett. **15**, 327 (1969).

[26] S. Logothetidis, J. Petalas, M. Cardona, and T. D. Moustakas, Phys. Rev. B **50**, 18 017 (1994).

[27] C. Kittel, *Quantum Theory of Solids*, 2nd ed. (Wiley, New York, 1987), Chap. 14.

[28] *Zahlenwerte und Funktionen aus Naturwissenschaften und Technik*, edited by O. Madelung and M. Schulz, Landolt-Börnstein, New Series, Group III, Vol. 22, pt. a (Springer, New York, 1987).

[29] E. Ortega and F. J. Himpsel, Phys. Rev. B **47**, 2130 (1993).

[30] R. R. Zucca and Y. R. Shen, Phys. Rev. B **1**, 2668 (1970).

[31] W. E. Spicer and R. C. Eden, *Proceedings of the Ninth International Conference on the Physics of Semiconductors, Moscow, 1968* (Nauka, Leningrad, 1968), Vol. 1, p. 61.

[32] A. L. Wachs, T. Miller, T. C. Hsieh, A. P. Shapiro, and T. C. Chiang, Phys. Rev. B **32**, 2326 (1985).

[33] R. A. Forman, W. Thurber, and D. E. Aspenes, Solid State Commun. **14**, 1007 (1974).

[34] R. Hulthen and N. G. Nilsson, Solid State Commun. **18**, 1341 (1976).

[35] D. Straub, L. Ley, and F. J. Himpsel, Phys. Rev. Lett. **54**, 142 (1985).

[36] D. E. Aspenes and A. A. Studna, Solid State Commun. **11**, 1375 (1972).

[37] F. J. Himpsel, J. F. van der Veen, and D. E. Eastman, Phys. Rev. B **22**, 1967 (1980).

[38] R. A. Roberts and W. C. Walker, Phys. Rev. **161**, 730 (1967).

[39] F. R. McFeeley, S. P. Kowalczyk, L. Ley, R. G. Cavell, R. A. Pollak, and D. A. Shirley, Phys. Rev. B **9**, 5268 (1974).

[40] K. M. Glassford and J. R. Chelikowsky, Phys. Rev. B **47**, 1732 (1993).

[41] K. Schwarz, Phys. Chem. Miner. **14**, 315 (1987).

[42] M. S. Hybertsen and S. G. Louie, Phys. Rev. Lett. **55**, 1418 (1985); Phys. Rev. B **34**, 5390 (1986).

[43] M. Rohlfing, P. Krüger, and J. Pollmann, Phys. Rev. B **48**, 17 791 (1993).

[44] W. Schöne and A. G. Eguiluz, Phys. Rev. Lett. **81**, 1662 (1998).

[45] V. L. Moruzzi, J. F. Janak, and A. R. Williams, *Calculated Electronic Properties of Metals* (Pergamon, New York, 1978).

[46] P. Hohenberg and W. Kohn, Phys. Rev. **136**, B864 (1964).

[47] W. Kohn and L. J. Sham, Phys. Rev. **140**, A1133 (1965).

[48] A. K. Rajagopal and J. Callaway, Phys. Rev. B **7**, 1912 (1973). See also, M. V. Ramana and A. K. Rajagopal, Phys. Rev. A **24**, 1689 (1981).

[49] See, J. P. Perdew and Alex Zunger, Phys. Rev. B **23**, 5048 (1981); **33**, 8800 (1986); **33**, 8822 (1986).